

Haverford College

## Haverford Scholarship

---

Faculty Publications

Physics

---

1994

### Nanofabrication and Rapid Imaging with a Scanning Tunneling Microscope

S. Rubel

M. Trochet

E. E. Ehrichs

Walter Fox Smith

*Haverford College*, [wsmith@haverford.edu](mailto:wsmith@haverford.edu)

Follow this and additional works at: [https://scholarship.haverford.edu/physics\\_facpubs](https://scholarship.haverford.edu/physics_facpubs)

---

#### Repository Citation

Rubel, S., et al. "Nanofabrication and rapid imaging with a scanning tunneling microscope." *Journal of Vacuum Science & Technology B* 12.3 (1994): 1894-1897.

This Journal Article is brought to you for free and open access by the Physics at Haverford Scholarship. It has been accepted for inclusion in Faculty Publications by an authorized administrator of Haverford Scholarship. For more information, please contact [nmedeiro@haverford.edu](mailto:nmedeiro@haverford.edu).

## Nanofabrication and rapid imaging with a scanning tunneling microscope

S. Rubel, M. Trochet, E. E. Ehrichs, W. F. Smith, and A. L. de Lozanne

Citation: *J. Vac. Sci. Technol. B* **12**, 1894 (1994); doi: 10.1116/1.587664

View online: <http://dx.doi.org/10.1116/1.587664>

View Table of Contents: <http://avspublications.org/resource/1/JVTBD9/v12/i3>

Published by the AVS: Science & Technology of Materials, Interfaces, and Processing

### Additional information on *J. Vac. Sci. Technol. B*

Journal Homepage: <http://avspublications.org/jvstb>

Journal Information: [http://avspublications.org/jvstb/about/about\\_the\\_journal](http://avspublications.org/jvstb/about/about_the_journal)

Top downloads: [http://avspublications.org/jvstb/top\\_20\\_most\\_downloaded](http://avspublications.org/jvstb/top_20_most_downloaded)

Information for Authors: [http://avspublications.org/jvstb/authors/information\\_for\\_contributors](http://avspublications.org/jvstb/authors/information_for_contributors)

## ADVERTISEMENT

# Instruments for advanced science

**Gas Analysis**



- dynamic measurement of reaction gas streams
- catalysis and thermal analysis
- molecular beam studies
- dissolved species probes
- fermentation, environmental and ecological studies

**Surface Science**



- UHV TPD
- SIMS
- end point detection in ion beam etch
- elemental imaging - surface mapping

**Plasma Diagnostics**



- plasma source characterization
- etch and deposition process reaction kinetic studies
- analysis of neutral and radical species

**Vacuum Analysis**




- partial pressure measurement and control of process gases
- reactive sputter process control
- vacuum diagnostics
- vacuum coating process monitoring

contact Hiden Analytical for further details

**HIDEN ANALYTICAL**

[info@hideninc.com](mailto:info@hideninc.com)  
[www.HidenAnalytical.com](http://www.HidenAnalytical.com)

CLICK to view our product catalogue 

# Nanofabrication and rapid imaging with a scanning tunneling microscope

S. Rubel, M. Trochet,<sup>a)</sup> E. E. Ehrichs,<sup>b)</sup> W. F. Smith,<sup>c)</sup> and A. L. de Lozanne<sup>d)</sup>

Department of Physics, The University of Texas at Austin, Austin, Texas 78712-1081

(Received 9 August 1993; accepted 28 January 1994)

Nanowires have been made by decomposing organometallic gases in a UHV scanning tunneling microscope (STM); this process is a form of chemical vapor deposition (CVD). Our STM is coupled to a commercial scanning electron microscope (SEM), which allows us to align the tip with pre-existing contact pads for electrical measurements of the nanowires. Thus four-contact measurements on two wires have been performed, a first for STM-fabricated structures. The resistivity of the first wire made from a nickel carbonyl precursor gas is  $34 \pm 10 \mu\Omega \text{ cm}$  at room temperature. This is remarkably close to the bulk value of  $7.8 \mu\Omega \text{ cm}$ , since the wire is only 5 nm thick, 190 nm wide and  $3.7 \mu\text{m}$  long. This indicates that the nickel deposits are fairly pure, and is consistent with Auger analysis made on micron-size deposits: there is at least 95% nickel in these deposits. This is a substantial improvement over previous results from our group and the few other groups using this technique. The second wire is  $1.45 \mu\text{m}$  long and 100 nm wide; its thickness is estimated at 5 nm. It has substantially higher resistivity:  $1.1 \pm 0.45 \text{ m}\Omega \text{ cm}$ , which is attributed to minute near discontinuities in the wire. Finally, lines have been written 4 nm thick, 35 nm wide, and  $2 \mu\text{m}$  long, which are unfortunately not long enough to allow resistivity measurements. Reliability problems of this complex STM/SEM system are discussed and new designs for a more dependable system are described. A new technique for rapid imaging of large areas ( $10\text{--}20 \mu\text{m}^2$ ) with the STM is being developed and preliminary results are presented here.

## I. INTRODUCTION

As the push to explore the behavior of mesoscopic systems continues, the need for a reliable, cost-effective, and readily available lithography system has grown apace. Fortunately, high throughput is not required in applications such as basic research or the repair of lithographic masks. Here, scanning tunneling microscope (STM) fabrication techniques using existing technology offer an attractive, low-cost approach. As a new technology, STM nanofabrication is still proving itself in two critical areas: repeatability and ultimate resolution. In this paper, we discuss these issues and our success with them, as well as directions for further improvement.

## II. DESCRIPTION OF STM-CVD AND RESULTS

Our technique is based on chemical vapor deposition (CVD), a process commonly used in the semiconductor industry to make thin films. We use similar precursor gases, but in our case we use the electrons from the STM tip to break down the precursor molecules. Thus the resolution of this technique is limited in principle only by the size of the precursor molecule. Dujardin *et al.*<sup>1</sup> have indeed shown that the STM can break down individual decaborane molecules.

Since our first demonstration of STM-CVD,<sup>2,3</sup> a few groups have used this nanofabrication technique to make structures in the 10- to 100-nm range.<sup>4-7</sup> The smallest (10 nm) were recently reported by Kent *et al.*<sup>7</sup> They used iron pentacarbonyl to make iron dots for studies of quantum magnetism.<sup>8</sup> They also grew very pure (less than 0.4% con-

tamination) iron filaments on their STM tip. A more complete review of STM-CVD is given in Ref. 9.

Since reporting the first four-point resistance measurement of a wire written by STM,<sup>10</sup> we have performed similar measurements on another wire  $1.45 \mu\text{m}$  long, 100 nm wide, and approximately 4 nm thick. Unlike the other two wires discussed in this article, however, we could not obtain AFM images, and instead were forced to use SEM photographs. While the lateral dimensions are accurate to within a few percent, the thickness is an estimate based on the (AFM-measured) dimensions of wires deposited under similar conditions. These parameters, similar to our previous report, were nickel carbonyl precursor at  $10^{-5}$  Torr, sample biased at +15 V, and writing speed of 10 nm/s. The resistance curve, shown in Fig. 1, bears a strong resemblance to that of our first lines. The silicon substrate dominates the high-temperature resistance, as discussed in detail in Ref. 10. At low temperatures, the conductivity rises exponentially, which is characteristic of a material with a small band gap. This material is presumably a nickel silicide. Most importantly, there is a relatively wide regime (110–160 K) in which the resistance rises linearly with temperature, characteristic of conduction in a metal. The temperature coefficient of resistance (40 ppm/K) is smaller by a factor of 4, which probably indicates that this wire is more disordered than the previous one.<sup>10</sup> We believe this disorder manifests because of height variations in the wire: small parts of it are narrow enough that they thoroughly dominate its resistance.

Both ourselves and others<sup>6</sup> have observed the somewhat "spotty" nature of lines produced by STM direct writing. Rather than producing smooth lines of uniform thickness, the STM tends to produce a closely spaced series of somewhat irregular dots. The thickness of a written line thus varies along its length. Since we perform our deposition at room

<sup>a)</sup>Present address: Motorola, Inc., Austin, TX.

<sup>b)</sup>Present address: James Franck Inst., Univ. of Chicago, Chicago, IL.

<sup>c)</sup>Present address: Dept. of Physics, Haverford College, Philadelphia, PA.

<sup>d)</sup>To whom correspondence should be addressed.

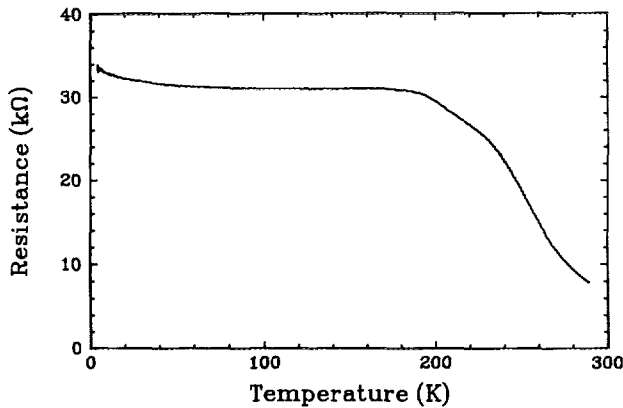


FIG. 1. Resistance vs temperature for a wire of approximate dimensions  $1.45 \mu\text{m} \times 100 \text{ nm} \times 4 \text{ nm}$  made by STM-CVD with a nickel carbonyl precursor.

temperature, the first fifteen monolayers or so of nickel promptly form the silicide  $\text{NiSi}_2$ . For lines as thin as ours (only 4 nm on average), it is quite plausible that only the silicide exists along certain sections; they will then dominate the conductivity at low temperatures. We note, however, that the resistivity of pure  $\text{NiSi}_2$  thin (10–100 nm) films is  $50 \mu\Omega \text{ cm}$  at room temperature.<sup>11</sup> This is not high enough to explain the resistivity of the second wire we measured without additional effects such as disorder or impurities.

Auger analysis of deposits written under similar conditions found them to be quite pure, with less than 5% carbon content and only trace amounts of oxygen.<sup>12</sup> Our film quality results primarily from moving to a UHV system (base pressure  $5 \times 10^{-10}$  Torr); Ref. 7 discusses the effect of some other process parameters. The good agreement between the resistivity of our first wire and the value for bulk nickel indicates that our levels of carbon contamination probably do not dramatically affect the conductivity. Since our process parameters have remained relatively constant, we have no reason to believe that our second wire contains significant amounts of carbon where the first did not. The effects of disorder and low dimensionality are not so clear however. Previous experiments on clean aluminum wires 25 nm thick and 200 nm wide showed one-dimensional behavior only as high as 15 K,<sup>13</sup> while our wires showed a significant resistance rise at 50 K. The much smaller dimensions of our wires should permit one-dimensional behavior to manifest at a higher temperature but nickel, unlike aluminum, is magnetic. The effect of magnetic scatterers on electron localization and the dimensionality of the system is unclear at this time, such systems being extremely difficult to treat theoretically.

Figure 2 shows one of our narrowest lines to date: 35 nm wide and 4 nm thick. Unfortunately, the line was too short for us to perform electrical measurements, but the fact that we wrote a relatively long ( $2 \mu\text{m}$ ) wire of such narrow width shows great promise for the technique. Clearly STMs can write features on the same length scales as more expensive systems such as electron beam lithography.

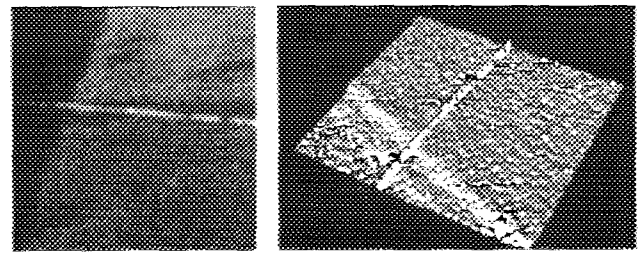


FIG. 2. AFM image,  $1.5 \mu\text{m}$  on a side, of a nickel wire written by STM-CVD with approximate dimensions of  $35 \text{ nm} \times 4 \text{ nm} \times 2 \mu\text{m}$ .

### III. NEW METHOD FOR IMAGING LARGE AREAS RAPIDLY

Throughput currently presents the fundamental obstacle to improving our performance. Bias voltage, writing speed, current, choice of precursor gas and pressure, tip material and preparation (with its own host of variables), and surface preparation present a dizzying number of combinations. Optimizing a process with this many variables requires performing a tremendous number of trials, even using shortcuts such as numerically generated fractional factorial (“*d*-optimal”) experiment designs. It is critical then for any group truly pushing the edge of nanolithography to have a system which can reproducibly perform lithography on a large number of samples.

Such, regrettably, is not the case with our current system. Designed as a prototype device, it was strongly constrained by the simultaneous need for ultrahigh vacuum operation and high (better than  $0.5 \mu\text{m}$ ) imaging resolution over a wide (up to  $5 \times 5 \text{ mm}^2$ ) area. The only feasible option at the time was the combined SEM/STM system, which has been described in detail elsewhere.<sup>12,14,15</sup> The system has successfully proved the viability of STM-CVD, but since then it has become apparent that we require a design with higher sample throughput.

Since we built our SEM/STM, long working distance (14–20 mm) optical microscopes with high resolution ( $\sim 1 \mu\text{m}$ ) have become available commercially at reasonable cost (e.g., from Nikon). We are now developing a new STM system which will place the tip and sample very close ( $\sim 8 \text{ mm}$ ) to a custom UHV window. We will then use an optical microscope to position the tip. Our new design will also eliminate the unreliable inchworm motors (Burleigh Instruments) we have used up to now. These motors’ piezo tube elements have shown themselves extremely susceptible to cracking, even when not subjected to transverse loads.

Because the resolution of the optical system is barely adequate for positioning our tip, we have developed a new imaging system. Employing field emission rather than tunneling current, we are able to combine submicron resolution with imaging at high speed over a large ( $4.2 \times 5.6 \mu\text{m}^2$ ) area. In preliminary experiments we have imaged at a rate of 6 s/frame, and we believe we will be able to obtain near TV rates (30 frames/s) in the near future using faster electronics. At this scanning speed we will be able to speedily position the tip relative to the contact pads, after first placing it in the right general vicinity using the optical microscope.

Our imaging system relies on differences in the field emission properties between the 30-nm-thick platinum contact pads and the (111) *n*-type silicon substrate when the sample is negative, and on the Schottky barrier formed between the contact pads and the silicon when the sample is positive. Crudely, we can model the field emission current density using the Fowler–Nordheim equation:

$$j = AE^2 \exp[-b\phi^{3/2}/E],$$

where  $A$  is a constant depending on the emitter,  $E$  is the electric field strength at the cathode (in V/nm),  $b$  is a universal constant equal to  $6.8 \text{ eV}^{-3/2} \text{ V/nm}$ , and  $\phi$  is the cathode's work function (in eV). Although it is a very crude model, describing field emission from perfectly clean metals, the Fowler–Nordheim equation does highlight the critical role the work function plays in field emission. Given the very different values for platinum and *n*-type silicon (5.65 and 4.85 eV, respectively<sup>16</sup>) the field emission current should change dramatically as a tip scans over different areas when the sample is biased negatively. On the other hand, when the sample is positive, the contrast is probably due to the presence of a Schottky barrier of 0.61 eV and the Cr–*n*Si interface.<sup>17</sup> (We use Cr as an adhesion layer between Pt and Si.)

In our microscope, we bias the sample relative to the tip, which is held at virtual ground. The signal runs into an amplifier (Burr–Brown OPA-111) located inside the vacuum chamber. Its proximity to the tip ( $\sim 2 \text{ cm}$ ) significantly reduces electrical noise and increases our bandwidth. This is the same preamplifier used for normal STM operation. Outside the vacuum chamber a high speed commercial amplifier (Princeton Applied Research, model 113) provides additional gain in order to display the signal on an oscilloscope. We use commercial electronics (RHK Technology, model STM 100) to drive the PZT-5H piezoelectric scanner tube (Stavely Sensors) which holds the sample.

Imaging with field emission is not new, in fact it even predates the STM, as can be seen in the pioneering work of Young *et al.*<sup>18</sup> Others have used STMs in the field emission mode more recently.<sup>19</sup> In all these cases feedback was used to keep a constant field emission current. Our idea is that at high voltage the tip is far from the surface (about 100 nm) so that a “constant height” mode is safe to use, thus allowing very rapid scans over large areas. The signal is then the current, since little or no feedback is used. Clearly, this is not meant for all types of samples and is only aimed at obtaining enough resolution for quick coarse positioning.

#### IV. RESULTS OF RAPID FIELD EMISSION IMAGING (RFEI)

Our initial imaging attempts were one-dimensional scans performed at high (+100 V) sample bias. Figure 3(a) shows an SEM photograph of the tip (and its shadow) just to the right of a roughly 750-nm-diam hole in the platinum contact pad. Figure 3(b) shows the 1.9- $\mu\text{m}$ -wide scan, with a 21 nA current spike at the location of the hole. The width of the hole in this scan is approximately 220 nm, less than that shown in the SEM photograph. This may be due to partial platinum coverage at the edge of the hole: the platinum-to-

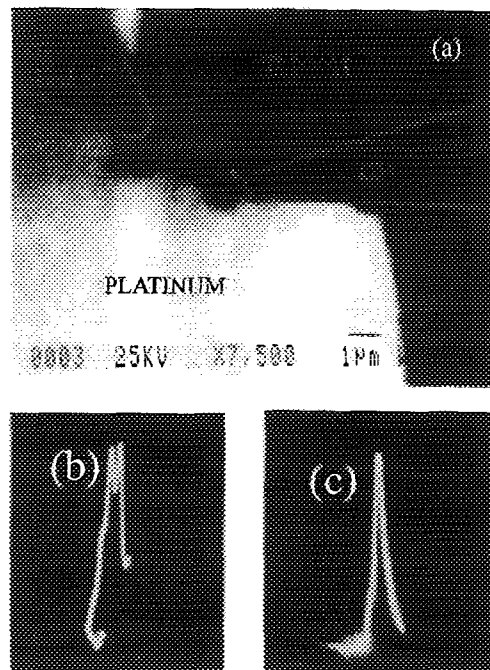


FIG. 3. (a) *In situ* SEM image of an STM tip aligned with the edge of a Pt contact pad. Rapid scanning in one dimension over this region in field emission mode clearly shows the position of the hole in the metal as a 21 nA spike in the emission current, 220 nm wide, as shown in (b). Panel (c) shows a 17 nA spike over the same hole which has now grown to a width of 260 nm. (The  $x$ -axis scale is different in the two line scans.)

bare-silicon transition was not sharp, and our backscattered electron detector is not sensitive to thin layers of materials due to the high energy of the incident SEM beam.

We then repeated the scan over a large range, 3.4  $\mu\text{m}$ . Again, we observed a large current spike (17.5 nA) in a location corresponding to the hole's position in the scan. The apparent width of the hole increased to 260 nm. This is not due to a change in the scan calibration, but instead to an actual widening of the hole, resulting from field evaporation of the platinum. The change in the hole was clearly visible in later SEM scans of the area (not shown). We emphasize that the resolution of the image is more than adequate for the purposes of positioning the tip over a desired area of the sample. Furthermore, the tip's scanning speed relative to the surface (19 and 33  $\mu\text{m/s}$  for Figs. 3(b) and 3(c), respectively) is roughly 1000 times faster than a typical STM scan. At these tip speeds a 256 line image could have been imaged in approximately 46 and 26 s, respectively.

We next moved the tip to a new, relatively undamaged area to perform a two-dimensional scan. We also lowered the sample bias to 20 V, at which point we observed no field evaporation of the platinum.

Figure 4 shows SEM and field emission scans of the area we imaged. Again, we were able to detect currents of approximately 20 nA over the silicon, with almost no current over the platinum areas (bright areas correspond to less current in the field emission image). We scanned the  $8.3 \times 11.3 \mu\text{m}^2$  image at a rate of 50 ms/line; the resulting tip speed relative to the surface was 166  $\mu\text{m/s}$ . At this high speed, we produced complete 256 line images in only 12.8 s. We also

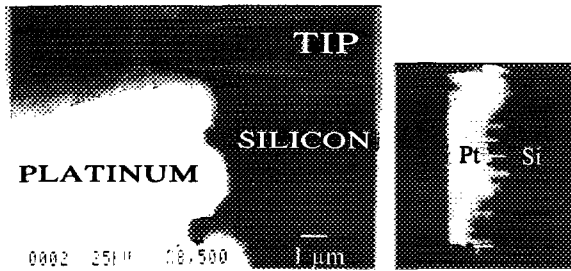


FIG. 4. *In situ* SEM image (left) of an STM tip aligned with the edge of a Pt contact pad. (b) Rapid field emission scanning in two dimensions over this region shows the edge of the metal very clearly. The 1  $\mu\text{m}$  bar in the SEM image gives the scale for both images.

obtained images at higher rates, but were not able to capture them on film.

With the recent arrival of an integrated scanning and display system (Nanoscope III, Digital Instruments), we acquired another field emission image of a contact pad edge as shown in Fig. 5. We did not make this particular scan at high speed (6.6  $\mu\text{m/s}$  tip velocity). Instead, our interest lay in the robustness of the imaging system. We were able to consistently obtain RFEI images despite the fact that the tip was severely crashed. In this image, the sample was biased negatively ( $-18.6$  V) relative to the tip, indicating that the contrast comes from the difference in work functions of the metal and the semiconductor, as discussed above. The relatively lax vacuum requirements and robustness of the system to tip crashes are two of the more attractive features of field emission imaging. Furthermore, we chose to use relatively large bias voltages and currents primarily to obtain a more robust signal. Depending on the sample and desired resolution, lower voltages and/or currents could certainly be used.

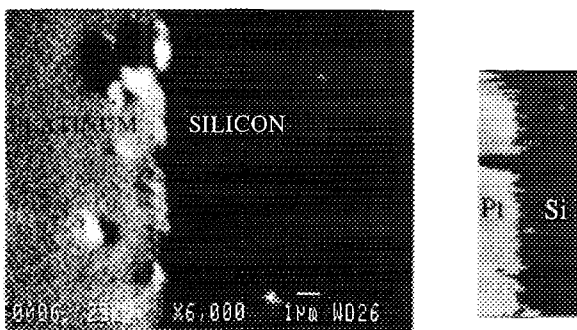


FIG. 5. Two-dimensional field emission image of the edge of a Pt contact pad. Some of the features along the edge are seen in both the SEM image (left) and STM field emission image (right). The 1  $\mu\text{m}$  marker gives the size scale of both images.

## V. CONCLUSIONS

We have described our latest results with STM-CVD and discussed reliability problems of our complex UHV STM/SEM. We have demonstrated a novel mode of STM operation, dubbed rapid field emission imaging, where the tip can scan large areas rapidly in order to locate particular features of the sample conveniently. We hope that RFEI will also be useful to other researchers in the STM field.

## ACKNOWLEDGMENTS

We would like to thank H. L. Edwards for his helpful advice, and C. K. Shih and D. Samara for the extended loan of their equipment. We gratefully acknowledge the support of the Air Force Office of Scientific Research, the Welch Foundation, the National Institute of Standards and Technology, and a Department of Education Fellowship (SR).

- <sup>1</sup>G. Dujardin, R. E. Walkup, and Ph. Avouris, *Science* **255**, 1232 (1992).
- <sup>2</sup>R. M. Silver, E. E. Ehrichs, and A. L. de Lozanne, *Appl. Phys. Lett.* **51**, 247 (1987).
- <sup>3</sup>E. E. Ehrichs, S. Yoon, and A. L. de Lozanne, *Appl. Phys. Lett.* **53**, 2287 (1988).
- <sup>4</sup>M. A. McCord, D. P. Kern, and T. H. P. Chang, *J. Vac. Sci. Technol. B* **6**, 1877 (1988).
- <sup>5</sup>M. A. McCord and D. D. Awschalom, *Appl. Phys. Lett.* **57**, 2153 (1990).
- <sup>6</sup>S. T. Yau, D. Saltz, and M. H. Nayfeh, *J. Vac. Sci. Technol. A* **9**, 1371 (1991).
- <sup>7</sup>A. D. Kent, T. Shaw, S. von Molnar, and D. D. Awschalom, *Science* **262**, 1249 (1993).
- <sup>8</sup>D. D. Awschalom, M. A. McCord, and G. Grinstein, *Phys. Rev. Lett.* **65**, 783 (1990).
- <sup>9</sup>A. L. de Lozanne, W. F. Smith, and E. E. Ehrichs, in *The Technology of Proximal Probe Lithography*, edited by C. Marrian (SPIE Optical Engineering Press, 1993), pp. 188–199; *Proc. NATO Workshop on Nanolithography*, edited by M. Gentili, C. Giovannella, and S. Selci (Kluwer Scientific, New York, 1994).
- <sup>10</sup>E. E. Ehrichs, W. F. Smith, and A. L. de Lozanne, *J. Ultramicrosc.* **42-44**, 1438 (1992).
- <sup>11</sup>S. M. Sze, *VLSI Technology*, 2nd ed. (McGraw-Hill, New York, 1988), p. 383.
- <sup>12</sup>W. F. Smith, E. E. Ehrichs, and A. L. de Lozanne, in *Nanostructures and Mesoscopic Systems*, edited by M. A. Reed and W. P. Kirk (Academic, New York, 1991), pp. 85–94.
- <sup>13</sup>D. Prober, S. Wind, and P. Santhanam, in *Localization, Interaction, and Transport Phenomena*, edited by B. Kramer, G. Bergmann, and Y. Bruynseraede (Springer, New York, 1985), pp. 148–161.
- <sup>14</sup>E. E. Ehrichs, W. F. Smith, and A. L. de Lozanne, *J. Vac. Sci. Technol. B* **9**, 1381 (1991).
- <sup>15</sup>E. E. Ehrichs, Ph.D. thesis, University of Texas at Austin, 1992.
- <sup>16</sup>*CRC Handbook of Chemistry and Physics*, edited by R. Weast, 64th ed. (CRC, Boca Raton, FL, 1984), p. E-77.
- <sup>17</sup>S. M. Sze, *Physics of Semiconductor Devices* (Wiley, New York, 1981), p. 291.
- <sup>18</sup>R. Young, J. Ward, and F. Scire, *Rev. Sci. Instrum.* **43**, 999 (1972).
- <sup>19</sup>See, for example, M. A. McCord and R. F. W. Pease, *J. Vac. Sci. Technol. B* **4**, 86 (1986); and also C. Marrian, E. Dobosz, and J. Dagata, *J. Vac. Sci. Technol. B* **10**, 2877 (1992).